UNIVERSITY OF LEIPZIG

Faculty of Physics and Earth Sciences
Institute of Experimental Physics I

GROUP “Molekülphysik”

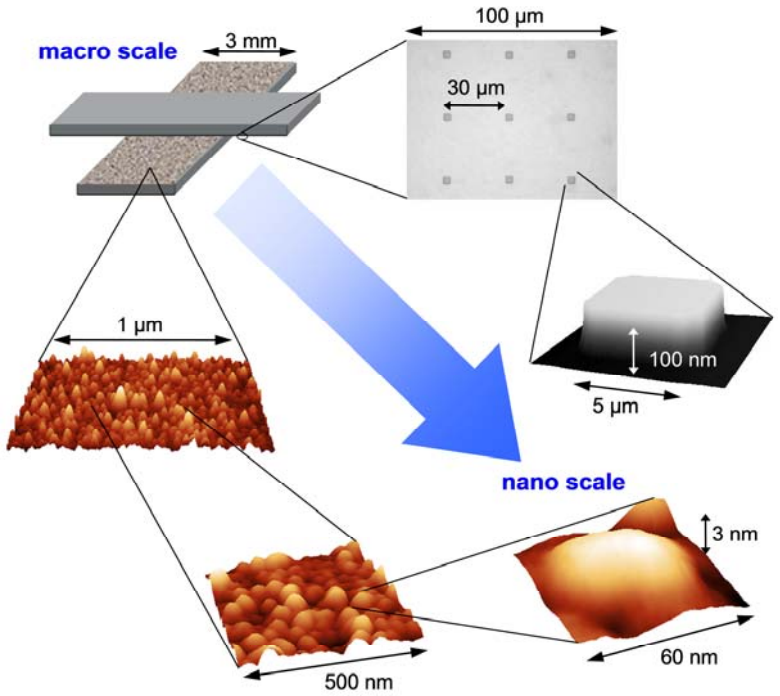

Annual Report 2010

Cover picture: Scheme of the sample capacitor built by crossed silicon wafer dice (top left); optical microscope and AFM pictures of the silica nano-structures with a heights of 100 nm (top and right) and a sub-layer of poly(2-vinyl pyridine) (bottom and left).

UNIVERSITÄT LEIPZIG
Fakultät für Physik und Geowissenschaften
Prof. Dr. Friedrich Kremer
Linnéstraße 5
04103 Leipzig
Germany

Tel.: (0341) 97-32550
FAX: (0341) 97-32599
E-Mail: kremer@physik.uni-leipzig.de

The year 2010

Tempora mutantur nos et mutamur in illis – times are changing and we are changing in it. While 5 – 10 years ago our group was the first to measure the molecular dynamics in polymer layers as thin as 10 – 20 nm, the focus has changed in the meantime to study molecular assemblies as thin as 1-2 nm and even isolated polymer coils. This could be achieved only due to the development of novel nanostructured electrode arrangements (s. cover page) which are now routinely used to determine by Broadband Dielectric Spectroscopy the molecular dynamics in extraordinary wide frequency and temperature ranges. As first result it was shown that the molecular mobility in the 1-dimensional confinement of thin polymer layers is bulk-like down to thicknesses smaller than 5 nm – a finding confirmed as well by Ellipsometry and Calorimetry. Many further highly promising experiments are on course, for instance to unravel the impact of the dimensionality of the geometrical constraints on the dynamics of glass-forming systems. - In our other main fields of activity, polarized time-resolved Fourier-Transform Infrared Spectroscopy and experiments with Optical Tweezers substantial progress was made. The structural levels of organization of spider silk are in the mean time quantitatively understood and the phenomenon of super-contraction in spider silk is well analyzed by deuteration experiments. Furthermore the novel technique of IR Transition Moment Orientational Analysis was developed and proven to be very versatile to analyze the mean orientation and the molecular order parameter of the different moieties in liquid crystalline polymers. In the experiments with Optical Tweezers great progress was made in various fields for instance in determination of the interaction potential between polymer brushes, in measurements on the electrophoretic mobility of *single* (polymer-grafted) colloids and refined studies on *single* receptor/ligand contacts. Recently an (HBFG)-application for the first commercially available Optical Tweezers set-up was positively approved.

January 2011 Friedrich Kremer

Contents

5. Graduations

Doctoral degree:

M. Sc. **J. R. Sangoro** "Rotational and translational diffusion in ionic liquids"

Dipl.-phys. **C. Gutsche** " Rheologische Untersuchungen an einzelnen Kolloiden mit Optischen Pinzetten"

Dipl.-phys. **K. Kegler** " Kraftmessungen zwischen DNS-beschichteten Kolloiden mittels Optischer Pinzetten"

Diploma

cand. phys. **C. Krause** "Charge transport and dipolar relaxations in imidazolium-based ionic liquids"

cand. phys. **T. Stangner** "Wechselwirkungskräfte zwischen Polymer-gepfropften Kolloiden"

6. Industry collaborations

Novocontrol
Hundsangen, Germany

Clariant Produkte (Deutschland) GmbH
Frankfurt am Main, Germany

Comtech GmbH
München, Germany

inotec FEG mbH
Markkleeberg, Germany

7. Patent applications

Deutsche Patentanmeldung Nr. 10 2005 045 065.2-54
Titel: "Detektorvorrichtung zur Funktionsprüfung von Dichtungssystemen"
Erfinder: Prof. Dr. F. Kremer

8. Awards

Prof. Dr. Friedrich Kremer was elected to give the Whitehead Memorial Lecture

page

1. Organization of the group

Leader: Prof. Dr. Friedrich Kremer

Academic Staff and Postdocs

Dr. Mahdy Elmahdy
Dr. Periklis Papadopoulos
Dr. Joshua Sangoro
Dr. Christof Gutsche

Students

Dipl. Phys. Tim Stangner
Dipl.-Phys. Olaf Ueberschär
Dipl. -Phys. Carolin Wagner
M. Sc. Ciprian Ghiorghita Iacob
Dipl.-Phys. Kati Kegler
Dipl.-Phys. Wilhelm Kossack
M. Sc. Wycliffe Kiprop Kipnusu
Dipl.-Phys. Christina Krause
M. Sc. Ilya Semenov
Dipl. Phys. Martin Tress
M. Sc. Emmanuel Mapesa
cand. phys. Tilman Schubert

Technical staff

Hartmut Domröse
Karin Girke
Ines Grünwald
Dipl.-Ing.(FH) Jörg Reinmuth
Dipl.-Phys. Wiktor Skokow
Dipl.-Phys. Cordula Babara Krause

Guests

Dr. Malgorzata Jasiurkowska

Alumni

Prof. Dr. Siegbert Grande

4. Financial support

Prof. Dr. F. Kremer

DFG-Projekt im Rahmen des Schwerpunktprogramms "Nano- und Mikrofluidik: Von der molekularen Bewegung zur kontinuierlichen Strömung" SPP 1164, KR 1138/14-3 (2006-2010)

Prof. Dr. F. Kremer

DFG-Projekt "Physicochemical characterisation of ionic liquids-mediated peptide acylation reactions" SPP 1191´, KR 1138/18-2 (2008–2010)

Prof. Dr. F. Kremer

DFG-Projekt "Charge transport and glassy dynamics in ionic liquids" SPP 1191, KR 1138/18-3 (2010–2012)

Prof. Dr. F. Kremer

DFG-Projekt "In-Situ Untersuchung der Wechselwirkungskräfte an Polyelektrolytbürsten", KR 1138/20-2 (2009–2011)

Prof. Dr. F. Kremer and Prof. Dr. K. Kroy

DFG-Projekt: "From local constraints to macroscopic transport: Dynamics of DNA under tension and confinement", FOR 877, KR 1138/21-1 (2007-2010)

Prof. Dr. F. Kremer

DFG-Projekt "Interfacial dynamics of polymers in interaction with solid substrates within the SPP "Polymer-Festkörper-Kontakte: Grenzflächen und Interphasen“, SPP 1369, KR 1138/23-2 (2010–2012)

Prof. Dr. F. Kremer

DFG-Projekt "Interfacial dynamics of polymers in interaction with solid substrates within the SPP "Polymer-Festkörper-Kontakte: Grenzflächen und Interphasen“, SPP 1369, KR 1138/23-1 (2008–2011)

Prof. Dr. F. Kremer is Principal Investigator and Lecturer in the International Research Training Group "Diffusion in Porous Materials" headed by **Prof. Dr. R. Gläser** and **Prof. Dr. F. Kapteijn**.

Prof. Dr. F. Kremer is Principal Investigator in the "Leipzig School of Natural Sciences – Building with Molecules and Nano-Objects" in the framework of a Graduate School funded by the **"Federal Excellence Initiative"**. This supports several Ph.D. projects.

15. Gutsche, C., M.M. Elmahdy, K. Kegler, I. Semenov, T. Stangner, O. Otto, O. Ueberschaer, U.F. Keyser, M. Krueger, M. Rauscher, R. Weeber, J. Harting, Y.W. Kim, V. Lobaskin, R.R. Netz, F. Kremer "Micro-Rheology on (Polymer-Grafted) Colloids Using Optical Tweezers" *Journal of Physics: Condensed Matter*, in press (2010)

2. Projects

2.1 Glassy dynamics of mono-molecular layers of poly(2-vinyl pyridine)

M. Tress, E. U. Mapesa, A. Serghei# and F. Kremer*

Recently, a preparation method using ultra-flat, highly doped silicon wafers as electrodes which are covered with strongly insulating silica nano-structures as spacers was developed in our group. This enables us to apply Broadband Dielectric Spectroscopy (BDS) to samples which do not exhibit a full surface coverage; in particular, the investigation of the glassy dynamics of ultra-thin layers of polymers down to and below the mono-molecular limit (where the polymer chains form sub-layers) is feasible [1]. In the case of poly(2-vinyl pyridine) (P2VP), it will be possible to study the dynamics of isolated coils which do not interact with each other and hence, can be treated as a statistical average over a single polymer chain in different conformations. First results reveal that in sub-layers with an average thickness of 3 nm neither the mean relaxation rate nor the shape of the relaxation time distribution function is changed compared to the bulk.

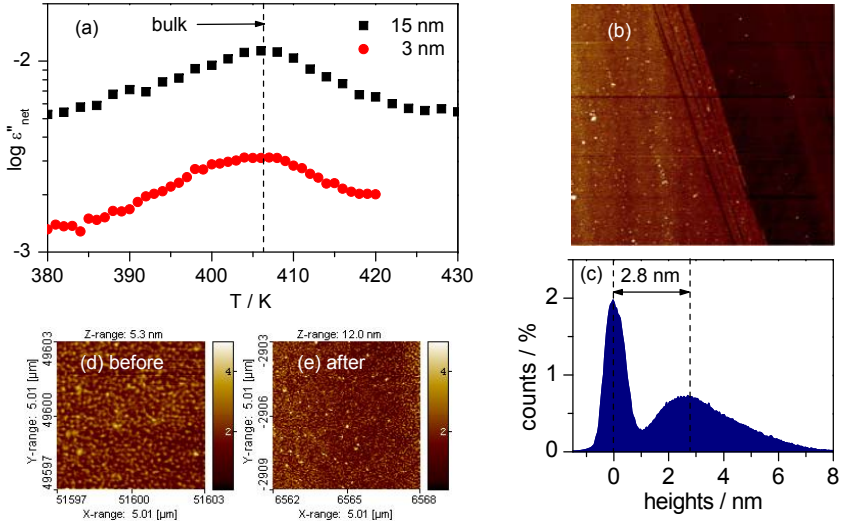

Fig. 1: a) Dielectric loss ε'' *versus* Temperature of two P2VP samples with thicknesses as indicated recorded at a frequency of 1.2 kHz. The α-relaxation peak coincides with the corresponding bulk value. b) and c) AFM picture (20 x 20 µm) and histogram of a scratch on the 3-nm-thick sample; the broad distribution of the heights of the polymeric surface indicates the characteristic of a sub-layer. d) and e) AFM pictures (5 x 5 µm^2) of the surface topology of the same sample taken before and after the measurement show the stability of the sample and especially the absence of dewetting; the corresponding values of the root mean square (RMS) roughness are 0.64 nm and 0.96 nm, respectively.

References:

[1] Tress, M., E. Erber, E. U. Mapesa, H. Huth, J. Müller, A. Serghei, C. Schick, K.-J. Eichhorn, B. Voit and F. Kremer, *Macromolecules*, 43 (2010) 9937-9944

Collaborators:

#Present address: Université Lyon 1, CNRS, Ingénierie des Matériaux Polymères, France
MicroFAB Bremen

Funding: Financial support by the BuildMoNa Graduate School is gratefully acknowledged.

* Underlining indicates the author who initiated the project.

2.2 Glassy dynamics and glass transition in nanometric thin layers of polystyrene

E. U. Mapesa, M. Tress, A. Serghei[#] and F. Kremer

In 2009, our group initiated an investigation on the glassy dynamics of ultra-thin (≥ 5 nm) layers of polystyrene (PS) by means of Broadband Dielectric Spectroscopy (BDS) and vis-Ellipsometry under identical and well controlled conditions for a wide range of molecular weights (58.9 kg/mol - 8090 kg/mol). First results examined no shift of T_g and no broadening in the glassy dynamics for PS layers as thin as 5 nm [1]. Recently, we extended this study by applying AC-calorimetry and X-ray reflectometry and confirmed our previous findings [2]. The characteristic temperature of the α-relaxation T_α as well as T_g of all molecular weights under study lies within a range of 4 K while the experimental error is as big as ± 2 K. Knowing about the strong impact of the sample preparation the present investigation emphasizes the identical preparation procedures in all applied methods and the resulting coincidence of the findings.

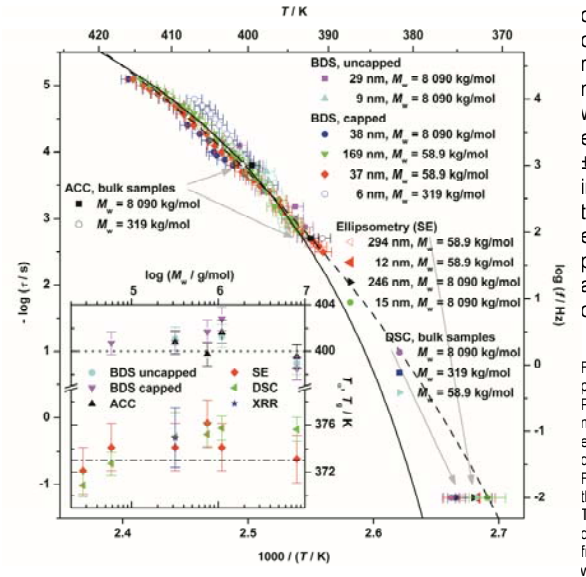

Fig. 1: Logarithm of the inverse relaxation time plotted *versus* inverse temperature for several PS samples (of diverse thicknesses and molecular weights) measured by different experimental methods as indicated. The dashed and solid lines are fits of the Vogel-Fulcher-Tammann equation to the BDS data of the 37 nm and 169 nm sample (58.9 kg/mol). The inset shows the molecular weight dependence of T_g and T_α (recorded at a frequency of 1 kHz) for bulk samples measured with different techniques.

References:
[1] Mapesa, E. U., M. Erber, M. Tress, A. Serghei, K.-J. Eichhorn, B. Voit and F. Kremer, *EPJ - ST*, 189 (2010) 173-180
[2] Tress, M., E. Erber, E. U. Mapesa, H. Huth, J. Müller, A. Serghei, C. Schick, K.-J. Eichhorn, B. Voit and F. Kremer, *Macromolecules*, 43 (2010) 9937-9944

Collaborators:
Ellipsometry, DSC: M. Erber, K.-J. Eichhorn, B. Voit, Institut für Polymerforschung Dresden (IPF)
X-ray reflectometry: J. Müller, M. Erber, K.-J. Eichhorn, B. Voit, IPF
Support for AC-Calorimetry: H. Huth, C. Schick, Universität Rostock

#Present address: Université Lyon 1, CNRS, Ingénierie des Matériaux Polymères, France
MicroFAB Bremen

Funding: DFG priority program SPP1369 (polymer-solid contacts: interfaces and interphases)

3. Publications

1. Krause, C., J.R. Sangoro, C. Iacob and F. Kremer "Charge transport and dipolar relaxations in imidazolium-based ionic liquids" *J. Phys. Chem. B,* **114**(1)**,** 382-386 (2010)
2. Papadopoulos, P., P. Heinze, H. Finkelmann, F. Kremer "Electromechanical properties of smectic C* liquid crystal elastomers under shear" *Macromolecules* **43** (16) 6666-6670 (2010) DOI:10.1021/ma1005028
3. Serghei, A., J. Lutkenhaus, D. Miranda, K. McEnnis, F. Kremer, T.P. Russel "Density fluctuations and phase transitions of ferroelectric polymer nanowires" *Small* **Vol. 6**,16 1822-1826 (2010) DOI: 10.1002/smll.201000562
4. C. Iacob, J. R. Sangoro, P. Papadopoulos, T. Schubert, S. Naumov, R. Valiullin, J. Kärger, and F. Kremer "Charge transport and diffusion of ionic liquids in nanoporous silica membranes" *Phys. Chem. Chem. Phys.* **12**, p.13798-13803 (2010), DOI:10.1039/c004546b
5. Mapesa, E.U., M. Erber, M. Treß, K.-J. Eichhorn, A. Serghei, B. Voit and F. Kremer "Glassy dynamics in nanometer thin layers of polystyrene" *Europ. Phys. J. - Special Topics* **189**, 173-180 (2010), DOI: 10.1140/epjst/e2010-01320-2
6. Erber, M., M. Treß, E.U. Mapesa, A. Serghei, K.-J. Eichhorn, B. Voit and F. Kremer "Glassy dynamics and glass transition in thin polymer layers of PMMA deposited on different substrates" *Macromolecules* **43**, 7729 (2010), DOI: 10.1021/ma100912r
7. Ene, R., P. Papadopoulos, F. Kremer "Partial deuteration probing structural changes in supercontracted spider silk" P*olymer* **51**, 21, 4784-4789 (2010) DOI:10.1016/j.polymer.2010.08.061
8. Drechsler, A., A. Synytska, P. Uhlmann, M. M. Elmahdy, M. Stamm, F. Kremer "Interaction forces between microsized silica particles and weak polyelectrolyte brushes at varying PH and salt concentration" *Langmuir* **26** (9) 6400-6410 (2010) DOI:10.1021/la904103z
9. Treß, M, M. Erber, E.U. Mapesa, H. Huth, J. Müller, A. Serghei, C. Schick, K.-J. Eichhorn, B. Voit and F. Kremer "Glassy Dynamics and Glass Transition in Nanometric Thin Layers of Polystyrene" *Macromolecules* **43**, 9937-9944 (2010) DOI: 10.1021/ma102031k
10. Elmahdy, M., C. Gutsche, F. Kremer "Forces within single pairs of charged colloids in aqueous solutions of ionic liquids as studied by optical tweezers" *J Phys Chem. C* **114**, 19452-19458 (2010)
11. W. Kossack, P. Papadopoulos, P. Heinze, H. Finkelmann, F. Kremer "Transition Moment Orientation Analysis on a Smectic C Liquid Crystalline Elastomer film" *Macromolecules* **43**, 18, 7532-7539 (2010), DOI:10.1021/ma101121f
12. Semenov, P. Papadopoulos, G. Stober, and F. Kremer "Ionic concentration- and pH-dependent electrophoretic mobility as studied by Single Colloid Electrophoresis" *J. Phys.: Condens. Matter* **22**, 494109 (2010)
13. Zech,O., J. Hunger, J.R. Sangoro, C. Iacob, F. Kremer, W. Kunz, R. Buchner "Correlation between polarity parameters and dielectric properties of [Na][TOTO] – a sodium ionic liquid" *Phys. Chem. Chem. Phys.* **12**, 14341-14350 (2010) DOI:10.1039/c0cp00840k
14. Turky, G., J.R. Sangoro, M. Abdel-Rehim, F. Kremer" Secondary Relaxations and Electrical Conductivity in Hyperbranched Polyester Amides" *J. Polym. Sci. B: Polym. Phys.* **48**,14, 1651-1657 (2010)

2.18 Single colloid electrophoresis on DNA-grafted colloids.

I.Semenov, P.Papadopoulos and F.Kremer

The novel method of Single Colloid Electrophoresis (SCE) [1,2] is applied to determine the electrophoretic mobility of single blank and DNA-grafted colloids. For that Optical tweezers are employed to measure separately the complex electrophoretic mobility of a single colloid and the complex electroosmotic response of the surrounding medium. For the bare particles pronounced effects are observed in dependence on concentration and valency of the ions in the surrounding medium and on its pH. For monovalent KCl solutions for instance a peak of the electrophoretic mobility at low concentrations is found (Fig.1) which agrees well with the predictions of the standard electrokinetic model [3]. For trivalent LaCl3 solutions at high concentrations charge inversion of the colloid as a whole takes place.
SCE is extended to polyelectrolyte-grafted colloids. This enables one to determine (Fig.1) for the first time the electrophoretic mobility of soft (DNA-grafted) particles under conditions of varying concentration and valency of the ions in the surrounding medium and to compare with the predictions of an approach suggested by Hill and Saville [4].

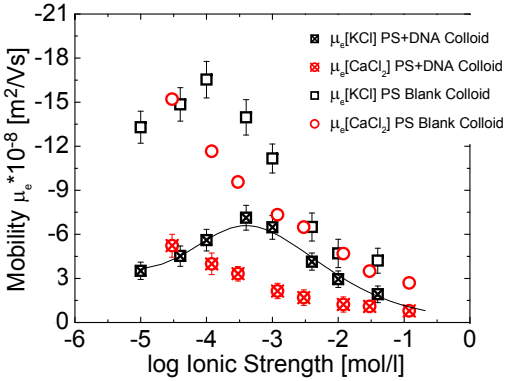

Fig. 1: Electrophoretic mobility vs. ionic strength of KCl and $CaCl_2$ aqueous solutions for a single DNA grafted (4000 bps, 1250 molecules per colloid) and similar blank negatively charged PS colloid (diameter: 2.0 µm). Laser power 0.2 W. Electric AC field frequency 12.5 Hz. For comparison the electrophoretic mobility in KCl solutions predicted by the Hill and Saville approach is displayed (solid line).

References:

[1] I. Semenov *et al.*, Journal of Colloid and Interface Science **337**, 260 (2009).
[2] O. Otto *et al.*, Review of Scientific Instruments **79**, 023710 (2008).
[3] I. Semenov *et al.*, Journal of Physics: Condensed Matter **22**, 494109 (2010).
[4] R. J. Hill, and D. A. Saville, Colloid Surf. A-Physicochem. Eng. Asp. 267, 31 (2005).

Funding: Sächsische Forschergruppe FOR 877, DFG.

2.3 Glassy dynamics in thin layers of cis-polyisoprene

E. U. Mapesa, M. Tress and F. Kremer

Broadband Dielectric Spectroscopy (BDS) – in combination with a nanostructured electrode arrangement – is used to study thin layers of cis-1,4-polyisoprene. From the viewpoint of BDS, polyisoprene belongs to a special type of polymers because a part of its molecular dipole moment attached to each monomer unit is aligned along the main chain. This fraction adds up to one dipole moment of the whole polymer chain corresponding to the end-to-end vector of the molecule. This enables the investigation of two distinct relaxation modes taking place at two different length scales: the segmental motion which involves structures of about one nanometer in size (2 to 3 monomer units) and the normal mode which represents the dynamics of the whole macromolecule. Previous studies [1-3] involved the evaporation of a metal counter-electrode onto the spin-cast layer. As a result of this (sandwich) geometry, a confinement-induced mode shows up between the normal and segmental modes, and gains dielectric strength with reducing film thickness at the expense of that of the normal mode. In the current study – where highly insulating silica nanostructures are used as spacers – one interface is free. The spin-cast samples are checked before and after dielectric measurement so that any dewetted layers are excluded from this study (Fig. 1). Down to 7 nm, it is observed (Fig. 2) that: (i) the segmental mode as a local relaxation process is unaffected by the 1-D confinement; (ii) the normal mode becomes faster with decreasing layer thickness; (iii) the normal mode gains dielectric strength with reducing layer thickness; and (iv) the so-called confinement-induced mode does not show up. For a quantitative analysis of these intriguing observations, simulations are planned to be carried out where the chain is treated as an ideal random walk in 3-D taking place between one penetrable and one impenetrable wall. Furthermore, a variation of the molecular weight is envisioned.

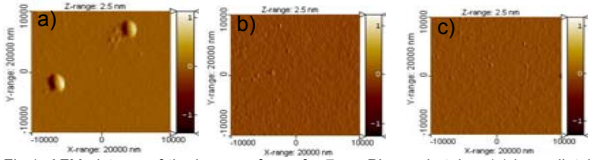

Fig.1: AFM pictures of the layer surface of a 7-nm PI sample taken (a) immediately after spin-casting, (b) after annealing in high oil-free vacuum before dielectric measurement and (c) after dielectric measurement. The root mean square roughness values are 2.4, 1.9 and 1.8 nm, respectively, showing that the surface remains unchanged during measurement.

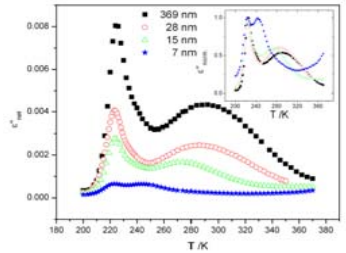

Fig. 2: Net dielectric loss ε''_{net} *versus* temperature at a frequency of 80 Hz for polyisoprene (molecular weight M_w = 53 kg/mol) in thin layers with thicknesses as indicated. Inset: same data normalized with respect to the maximum value of dielectric loss of the segmental mode.

References:

[1] A. Serghei and F. Kremer, Phys. Rev. Lett. 9**1**, 165702-1 (2003)
[2] A. Serghei, F. Kremer and W. Kob, Eur. Phys. J. E. **12**, 143 (2003)
[3] E.U. Mapesa, M. Erber, M.Tress, K.J. Eichhorn, A. Serghei, B. Voit and F. Kremer, Eur. Phys. J.-ST. **189**, 173 (2010)

Funding: Funding by DFG priority program SPP1369 (polymer-solid contacts: interfaces and interphases) is highly appreciated.

2.4 Molecular dynamics of *cis*-polyisoprene under geometrical confinement

W. K. Kipnusu, E.U. Mapesa, C. Iacob, J.R. Sangoro and F.Kremer

Broad-band dielectric spectroscopy is employed to study *cis* 1,4 polyisoprene. In the bulk state two distinct molecular processes are observed. The normal mode process due to dipole component parallel to the chain contour appears at higher temperatures (lower frequencies) and is proportional to the correction function of the fluctuations of the end-to-end vector of the whole polymer chain. Segmental mode which appears at lower temperatures (higher frequencies) as shown in Fig. 1, is associated to the dynamic glass transition. Both of the two processes are proportional to the monometric friction coefficients [1] and hence have the same temperature dependence as seen on the inset of Fig 1. A counterbalance between finite-size effects and surface effects are expected to influence molecular dynamics of these processes when the polymer melt is confined in cylindrical nanopores especially when the pore diameter is less than the radius of gyration of the polymer. From previous studies it is noted that the confinement effects is strongly dependent on the topology and dimensionality of the confining matrices [2,3,4]. In the current study [5], 2-D confinement of *cis*- 1,4 polyisoprene in unidirectional nanoporous silica matrices will be compared with 1-D confinement in spin cast thin films where silica nanostructures are used as spacers leaving one interface free. Nanoporous silica matrices are obtained after oxidation of porous silicon prepared by anodization of highly *p*- doped (100) oriented silicon substrates in HF electrolyte solution. This process leads to highly anisotropic pores running perpendicular to the surface of the wafer (Fig. 2a). Self- diffusion coefficients of *cis* 1,4 polyisoprene in bulk state and when confined in the nanoporous host systems will also be probed using both dielectric spectroscopy and pulse field gradient NMR spectroscopy.

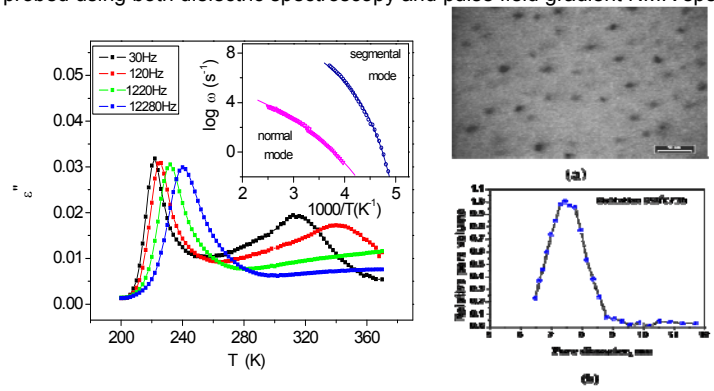

Fig.1: Dielectric loss *versus* temperature at the indicated frequencies for bulk cis 1,4 polyisoprene (Mw=53kg/mole). The inset shows temperature dependence of the segmental and the normal modes- lines represents the VFT fits. Fig. 2: (a) SEM image of the surface of porous silica. (b) Pore size distribution of the porous silica obtained from NMR cryoporometry.

References:
[1] K. Kojio, S. Jeon and S. Granik, Eur.Phys.J.E. 8 167 (2003)
[2] A. Serghei and F. Kremer, Phy.Rev. Lett. 91, 165702-1 (2003)
[3] R. Kimmich and N. Fatkullin, Macromolecules, in press (2011)
[4] P. Floudas and G. Fleischer, Europhys.Lett., 40 (6) 685(1997)
[5] W.K. Kipnusu, E.U. Mapesa, C. Iacob, J.R. Sangoro and F. Kremer, in preparation

Collaborators: J. Kärger, R. Valiullium (U Leipzig)

Funding: Financial support from DFG (Germany) and NOW (The Netherlands) within IRTG "Diffusion in Porous Materials" is highly appreciated.

2.16 The effective hydrodynamic radius of single DNA-grafted colloids as measured by fast Brownian motion analysis

O. Ueberschär, C. Wagner, T. Stangner, C. Gutsche and F. Kremer

Optical tweezers accomplished with fast position detection enable one to carry out Brownian motion analysis of *single* DNA-grafted colloids (grafting density: ~1000 molecules per particle, molecular weight: 4000 bp) in media of varying NaCl concentration. By that the effective hydrodynamic radius of the colloid under study is determined and found to be strongly dependent on the conformation of the grafted DNA chains. Our results compare well both with recent measurements of the pair interaction potential between DNA-grafted colloids (Kegler *et al.* [2]) and with microfluidic studies (Gutsche *et al.* [3]). The observed scaling of the brush height with the ion concentration is in full accord with the pertinent theoretical predictions by Pincus, Birshtein and Borisov.

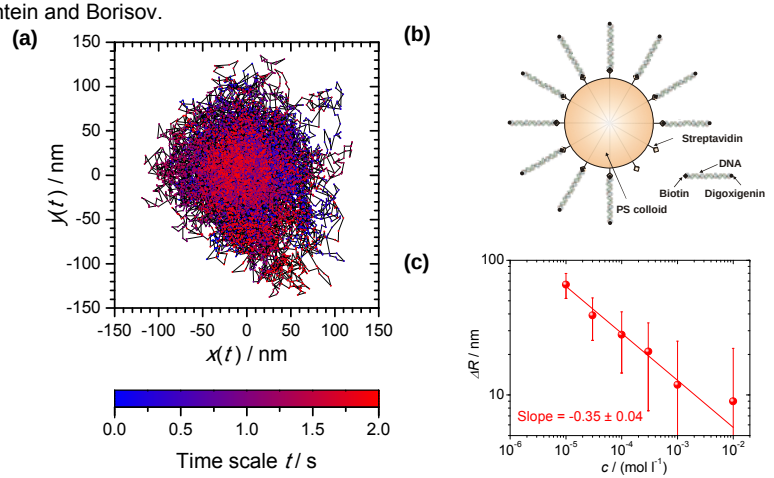

Fig. 1: (a) The centre of the colloid as determined by our two-dimensional intensity profile fit is subject to Brownian motion, which becomes apparent from the depicted trajectory. (b) Schematic of a streptavidin-coated microsphere to which DNA molecules are grafted. (c) The increase ΔR of the hydrodynamic radius with respect to different NaCl concentrations as measured for a *single* DNA-grafted colloid in the salted regime (to logarithmic scale). The linear fit of ΔR vs. the NaCl concentration c yields a power law scaling $\Delta R \propto c^{-\gamma}$ with an exponent of $\gamma = 0.35 \pm 0.04$. The molecular weight of the DNA molecules is 4000 base pairs. The reversibility of the salt-induced conformational change of the DNA brush as reflected in ΔR has successfully been verified.

References
[1] O. Ueberschär, C. Wagner, T. Stangner, C. Gutsche, F. Kremer, *submitted to* Polymer (November 2010)
[2] K. Kegler, M. Konieczny, G. Dominguez-Espinosa, C. Gutsche, M. Salomo, F. Kremer, C. N. Likos, Phy Rev Lett 100, 118302 (2008)
[3] C. Gutsche, M. Salomo, Y. W. Kim, R. R. Netz, F. Kremer, Microfluid Nanofluid 2, 381-386 (2006)

Funding: Financial support by the BuildMoNa Graduate School is gratefully acknowledged.

2.16 Interaction forces between a single pair of charged colloids as measured by Optical Tweezers

C. Gutsche, T. Stangner, M. M. Elmahdy, and F. Kremer

Optical Tweezers are an excellent tool to investigate the interaction force between a single pair of spherical charged colloids (diameters: polystyrene 2.24 ± 0.02 µm; silica 4.85 ± 0.05 µm) [1,2,4]. The concentration dependence was recorded under different conditions e.g. varying salt concentration and valancy (see Fig. 1 (a-f)). The data are well described by Derjaguin-Landau-Verwey-Overbeek (DLVO) theory [2,3]. A comparison of the fitted *Z* and *R* among different colloidal pairs of PS with monovalent counterions reveals that the radii are virtually the same whereas the obtained charges range from $Z \approx 200\,000$ to 450 000. For a given pair of colloids, at an increasing counterion valence, the fitted radius *R* remains essentially constant whereas the fitted charge *Z* decreases [2,4]. For reasons of comparison, data for of silica colloids (diameter 4.85 ± 0.05 µm) are plotted in Fig. 1 (d-f) and show a similar valence dependence. We attribute the latter effect to the neglect of the small-ion correlations in the DLVO theory, which gain importance at increasing counterion valence. The neglect of those leads to an underestimation of screening of the colloids while the functional force–separation dependence is essentially preserved.

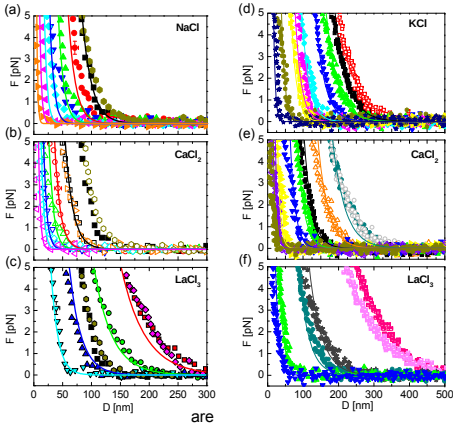

Fig. 1. (a-c) Force *F* vs. separation *D* for *one single* pair of Polystyrene (PS) colloids (diameter ~ 2.24 ± 0.02 *µm*) in aqueous solution of varying salt and salt concentrations from experiments (symbols) and the DLVO theory with fitted values of the parameters *Z* and *R* (curves). (a) NaCl at 0.3 mM (black squares), 0.55 mM (red circles), 1 mM (green triangles), 2 mM (blue nablas), 4 mM (cyan diamonds), 10 mM (magenta left triangles), and 30 mM (orange right triangles). To ensure a full reproducibility of the exchange of the medium and to exclude hysteresis effects due to possible adsorption effects on the colloids the sample cell was flushed again with 0.3 mM NaCl (gold diamonds). (b) $CaCl_2$ at 0.15 mM (black open squares), 0.3 mM (red open circles); 0.5 mM (green open triangles), 1 mM (blue open nablas), 1.5 mM (cyan open diamonds), 3 mM (magenta open left triangles), 0.15 mM (orange open right triangles), and finally 0.3 mM NaCl (gold open diamonds). (c) $LaCl_3$ at 3 *µM* (black red filled square), 10 *µM* (black green filled circle), 30 *µM* (black blue filled triangle), 100 *µM* (black cyan filled nablas), 3 *µM* (black magenta filled diamonds), and 0.3 mM NaCl solution (black gold filled diamonds). Some indicative error crosses are given. (d-f) Force *F* vs. separation *D* for a single pair of blank SiO_2 colloids (diameter ~ 4.85 ± 0.05 *µm*) in aqueous solution of varying salt and salt concentration from experiments (symbols) and the DLVO theory with fitted values of the parameters *Z* and *R* (curves). (d) Concentration dependence of KCl: 0.04 mM (black squares), 0.06 mM (green up-triangles), 0.1 mM (blue down-triangles), 0.2 mM (cyan diamonds), 0.3 mM (magenta left-triangles), 0.4 mM (yellow right-triangles), 1 mM (dark yellow diamonds), 4 mM (navy blue stars). To ensure the full reproducibility of the medium exchange, the cell was flushed again with 0.04 mM (open red squares). (e) Concentration dependence of $CaCl_2$: 0.01 mM (dark cyan circles and open grey circles for reproducibility), 0.02 mM (orange open up-triangles), 0.04 mM (black squares), 0.06 mM (green up-triangles), 0.1 mM (blue down-triangles), 0.4 mM (yellow right-triangles), 0.6 mM (violet crossed open squares) and 1 mM (dark yellow diamonds). (f) Concentration dependence of $LaCl_3$: 1 *µM* (pink half open up squares and light magenta half open down squares for reproducibility), 5 *µM* (grey open stars), 0.01 mM (dark cyan circles), 0.06 mM (green up-triangles) and 0.1 mM (blue down-triangles).

References:

[1] M.M. Elmahdy, A. Drechsler, C. Gutsche, A. Synytska, P. Uhlmann, F. Kremer, M. Stamm, *Langmuir* **25**, 12894 (2009)
[2] C. Gutsche, U.F. Keyser, K. Kegler, F. Kremer, Physical Review E **76**, 031403 (2007)
[3] B.V. Derjaguin, L. Landau, *Acta Physicochim. URSS* **14**, 633 (**1941)**
[4] C. Gutsche et al. JPCM accepted 2010

Funding: DFG priority program 1164 (Nano- & Microfluidics)

2.5 Rotational and translational diffusion in hyperbranched polyglycerols

T. Schubert, J. R. Sangoro, C. Iacob and F. Kremer

Dendritic polyglycerols are under intense investigation due to the wide range of applications envisaged in biomedical sciences and especially drug delivery. In the current study, rotational and translational diffusion in a series of hyperbranched polyglycerols (HPGs) are investigated by a combination of broadband dielectric spectroscopy (BDS), pulsed field gradient nuclear magnetic resonance (PFG NMR), rheology, frequency-dependent (ACC) as well as differential scanning calorimetry (DSC). The dielectric spectra are dominated by conductivity contribution at higher temperatures (and lower frequencies) whereas two closely adjacent secondary dipolar relaxation processes are observed at lower temperatures for all the samples investigated. Analysis of the real part of the complex dielectric function based on the Kramers-Kronig relations enables the separation of the latter. The slower dipolar relaxation is attributed to rotational diffusion – an assignment supported by rheological and calorimetric results. The Stokes-Einstein relation linking rotational and translational diffusion is shown to hold for the (low molecular weight) polymers investigated.

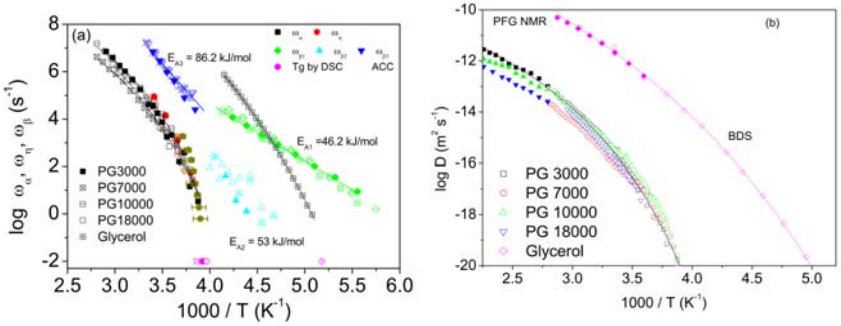

Fig. 1: (a) Thermal activation plot of the structural α-relaxation rates (squares) of polyglycerols with indicated molecular weights in g/mol (filled: 3000; crossed: 7000; dashed: 10000; open: 18000) in comparison to glycerol (crossed). The mechanical relaxation rates (circles) determined from rheology data are also shown. The secondary (β-) relaxation rates (triangles and diamonds) for the indicated molecular weights are also shown. Solid lines are fits by the Vogel-Fulcher-Tammann equation. (b) Temperature dependence of the diffusion coefficient as obtained from the structural α-relaxation (open) and PFG-NMR (filled) measurements for the given molecular weight. Logarithm is to base 10.

References:

[1] M. Calderón, M. A. Quadir, S. K. Sharma, and R. Haag (2010), Dendritic polyglycerols for biomedical applications. *Adv. Mater*. 22, 190-218
[2] J. R. Sangoro *et al*., Rotational and translational diffusion in hyperbranched polyglycerols, Under preparation.

Collaborators: R. Buchner (University of Regensburg), V. Strehmel (Niederrhein University of University of Applied Sciences), J. Kärger (University of Leipzig), R. Valliulin (University of Leipzig)

Funding: DFG under the priority program SPP 1191 on “Ionic Liquids”

2.6 Dielectric properties of ionic liquids: the effect of temperature *and* pressure

J. R. Sangoro and F. Kremer

Broadband dielectric spectroscopy is employed to investigate the influence of temperature *and* pressure on charge transport in ionic liquids (ILs). The dielectric spectra are dominated – on the low-frequency side – by electrode polarization effects while, for higher frequencies, charge transport in a disordered matrix is the underlying physical mechanism. Identical Vogel-Fulcher-Tammann-type dependence of the main quantities characterizing charge transport with respect to temperature *and* pressure is obtained (Fig. 1a). While the absolute values of dc conductivity and the characteristic charge transport rate vary over more than 10 decades with temperature, pressure and upon systematic structural variation of the ILs, a coinciding plot of the transport parameters is obtained (Fig. 1b). This is discussed within the framework of the concept of *glassy dynamics assisted charge transport* traced back to Einstein, Einstein-Smoluchowski, and Maxwell relations [1,2].

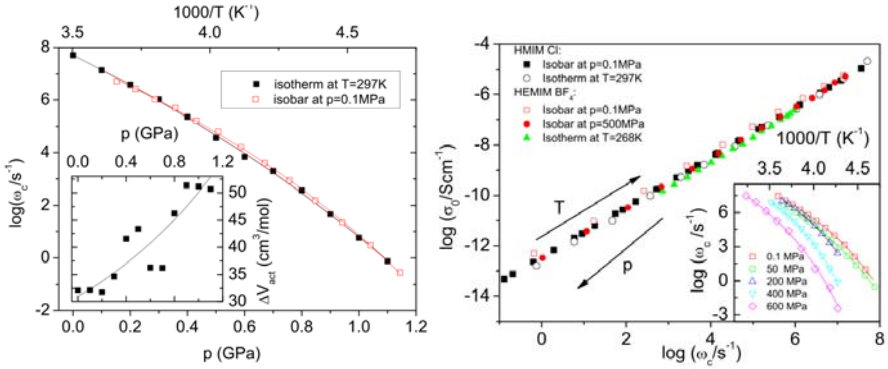

Fig. 1: (a) The characteristic rate of charge transport, ω_c, for the HMIM Cl ionic liquid at different pressure (isotherm) and as a function of inverse temperature (isobar). Inset: The apparent activation volume at different pressure as indicated. (b) The dc conductivity, σ_0, versus ω_c, for two ionic liquids as indicated. The data for all ionic liquids are obtained from dielectric measurements at ambient pressure except for the HMIM Cl for which the transport quantities are also measured at different pressures as indicated. This plot experimentally demonstrates the universality of charge transport in ionic liquids. The error bars are comparable to the size of the symbols, if not specified otherwise. Log is used to refer to logarithm to base 10.

References:

[1] *Broadband Dielectric Spectroscopy*, edited by F. Kremer and A. Schönhals, Springer (2003); J. R. Sangoro, A. Serghei, S. Naumov, P. Galvosas, J. Kärger, C. Wespe, F. Bordusa, and F. Kremer, Phys. Rev. E 77, 051202 (2008); J. R. Sangoro et al, J. Chem. Phys. 128, 214509 (2008); J. R. Sangoro, C. Iacob, A. Serghei, C. Friedrich, F. Kremer, *Phys. Chem. Chem. Phys*. 11, 913 (2009).
[2] J.R. Sangoro et al. (2011), under preparation

Collaborators: M. Paluch and M. Mierzwa (University of Silesia, Poland)

Funding: DFG under the priority program SPP 1191 on “Ionic Liquids”

2.15. Forces of interaction between grafted, blank and grafted-blank colloids by using optical tweezers

T. Stangner, M.M. Elmahdy, C. Gutsche and F. Kremer

The forces of interaction between blank SiO_2 colloids (diameter: ~ 4.85 ± 0.05 µm), poly (acrylic-acid) (PAA) grafted colloids and the asymmetric blank-grafted colloids are measured with high precision (± 50 fN) by means of Optical Tweezers. Parameters to be varied beside the surface modification are the concentration and the valency of the added salt. The Derjaguin-Landau-Verwey-Overbeek (DLVO) theory [1] is used for the characterization of the blank colloids. Good agreement was found (Fig. 1a). Therefore electrostatic contributions dominate the interaction [1,2]. The interaction between PAA-grafted colloids is characterized by a model published by Jusufi et al. including entropic parts to the overall interaction force (Fig. 1b). The asymmetric case, blank vs. grafted, was fitted by using the Alexander-De Gennes-Model (AdG model), which only take into account the steric force and non-charged colloids (Fig. 1c). Using the model-independent interaction length at a force of F=2 pN, the experimental results suggest that the interaction between the asymmetric case can be described as a superposition of half the interaction length of the blank and half of the interaction length of the grafted colloids (Fig. 1d).

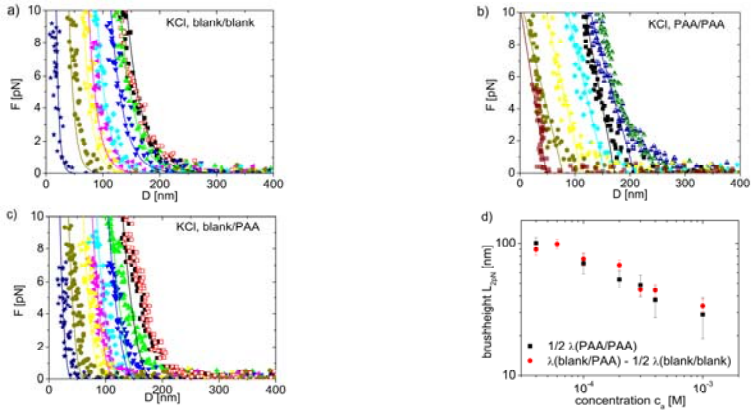

Fig. 1**:** a-c) Force *F* vs. separation *D* for three different pairs of SiO_2 colloids (diameter~4.85 ± 0.05 *µ*m) in aqueous solution (pH 7.3) of varying KCl concentration and surface modification from experiments (symbols). a) Concentration dependence for blank/blank: 0.04 mM (black squares), 0.06 mM (green up-triangles), 0.1 mM (blue down-triangles), 0.2 mM (cyan diamonds), 0.3 mM (magenta left-triangles), 0.4 mM (yellow right-triangles), 1 mM (dark yellow diamonds), 4 mM (navy blue stars). To ensure the full reproducibility of the medium exchange, the cell was flushed again with 0.04 mM (open red squares). The solid lines correspond to the fits using DLVO theory. b) Concentration dependence for PAA/PAA: 0 mM (half-open royal triangles and half-open olive triangles for reproducibility), 0.04 mM (black squares), 0.2 mM (cyan diamonds),0.4 mM (yellow right-triangles), 1 mM (dark yellow diamonds), 3 mM (open crossed wine red squares). The solid lines correspond to the fits using Jusufi theory. c) Concentration dependence for blank/PAA: 0.04 mM (black squares and open red squares for reproducibility), 0.06 mM (green up-triangles), 0.1 mM (blue down-triangles), 0.2 mM (cyan diamonds), 0.3 mM (magenta left-triangles), 0.4 mM (yellow right-triangles), 1 mM (dark yellow diamonds), 4 mM (navy blue stars). The solid lines correspond to the fits using AdG theory. d) Comparison between the model-independent brush height (half the interaction length) for PAA/PAA (black squares) and blank/PAA (red circles) in dependence of salt concentration. Both datasets coincide what suggests that the interaction between blank/PAA is dominated by electrostatic and entropic contributions.

References:

[1] C. Gutsche *et al.*, Physical Review E 76, 031403 (2007)
[2] C. Gutsche *et al*. JPCM accepted 2010

Funding: DFG Project (Project No. KR 1138/20-1, STA 324/33-1 (2007 - 2009))

2.14 Forces within single pairs of charged colloids in aqueous solutions of ionic liquids as studied by optical tweezers

M. M. Elmahdy, C. Gutsche and F. Kremer

Forces of interaction within *single* pairs of negatively charged microsized colloids in aqueous solutions of water miscible room temperature ionic liquids (RTILs) have been measured at varying concentrations and pH by using optical tweezers (OT) [1]. Three different water miscible RTILs (1-Butyl-3-methylimidazolium tetrafluoroborate [BMIM-BF4], 1-Butyl-3-methylimidazolium trifluoromethanesulfonate [BMIM-TfO] and 1-Butyl-3-methylimidazolium chloride [BMIM-Cl]) having the same organic cation $[BMIM]^+$ and different inorganic anions ($[BF4]^-$, $[TfO]^-$ and Cl^-) are used and compared with the high temperature molten salt (KCl). The experimental data are well described by a size-corrected screened Coulomb interaction approach which originates from the linearized Poisson-Boltzmann (PB) equation [2]. The effective surface charge density σ derived from the fitted force-separation data is found to be concentration and pH dependent.

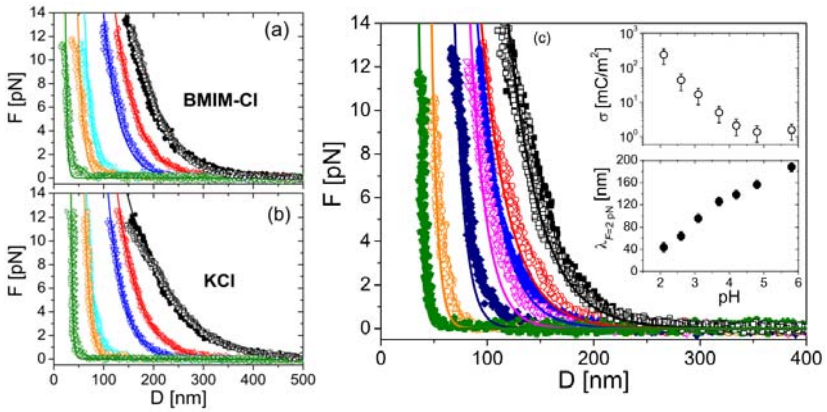

Fig 1: Forces *vs.* separation *D* as measured for a *single* pair of blank PS colloids in aqueous solution of two different types of salts (BMIM-Cl and KCl). Symbols represent the experimental data while the solid lines represent the fits with the size-corrected screened Coulomb interaction approach. (a) BMIM-Cl at fixed pH 5.8 and different concentrations: 2.2×10^{-5} M (black full circles), 5×10^{-5} M (red open up-triangles), 1×10^{-4} M (blue open down-triangles), 5×10^{-4} M (cyan open diamond), 1×10^{-3} M (orange open hexagon), 0.01 M (olive open right-triangles) and the reproducibility at 2.2×10^{-5} M (black open circles). (b) KCl at fixed pH 5.8 and different concentrations: 1.2×10^{-5} M (black full squares), 5×10^{-5} M (red open up-triangles), 1×10^{-4} M (blue open down- triangles), 5×10^{-4} M (cyan open diamond), 1×10^{-3} M (orange open hexagon), 0.01 M (olive open right-triangles), and the reproducibility check at 1.2×10^{-5} M (black open squares). (c) BMIM-Cl at fixed concentration of 1×10^{-4} M and different pH values of 2.1 (olive full pentagon), 2.6 (orange open hexagon), 3.1 (navy full diamond), 3.7 (magenta open down-triangles), 4.2 (blue full up-triangles), 4.8 (red open circles), 5.8 (black full squares) and the reproducibility at pH 2.1 (black open squares). Inset of (c): interaction length at force of 2 pN ($\lambda_{F=2\ pN}$) versus pH at fixed BMIM-Cl concentration of 1×10^{-4} M (black full circles). The pH-dependence of the effective surface charge density σ obtained from the fitting of the force separation curves.

References:

[1] M.M. Elmahdy, C. Gutsche, F. Kremer *J. Phys. Chem. C* **114**, 19452 (2010).
[2] C. Gutsche, U.F. Keyser, K. Kegler, F. Kremer *Physical Review E* **76**, 031403 (2007)

Funding: DFG priority program SPP 1191 on Ionic Liquids.

2.7 Diffusion in ionic liquids: the interplay between molecular structure and dynamics

J. R. Sangoro, C. Iacob and F. Kremer

Diffusion in a series of bis(trifluorosulfonyl)imide-based ionic liquids is investigated by a combination of Broadband Dielectric Spectroscopy (BDS) and Pulsed Field Gradient Nuclear Magnetic Resonance (PFG NMR). It is demonstrated that the mean jump lengths increase with the molecular volumes determined from quantum-chemical calculations. This provides a direct means – via Einstein-Smoluchowski relation – to determine the diffusion coefficient by BDS over more than 8 decades unambiguously and in quantitative agreement with PFG NMR measurements (see Fig. 1). Unprecedented possibilities in the study of charge transport and dynamic glass transition in ionic liquids are thus opened [1].

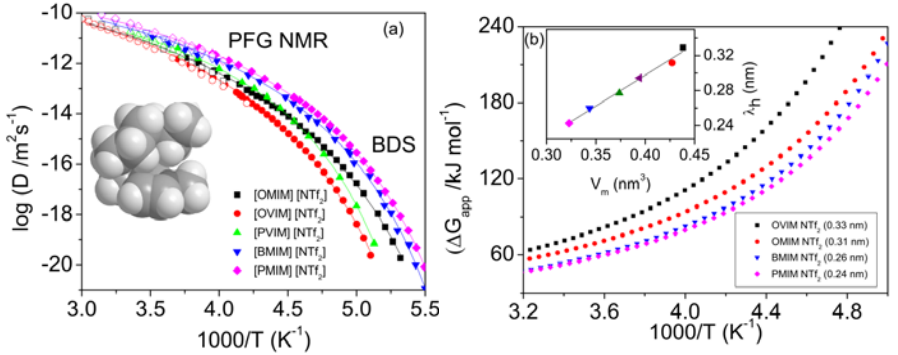

Fig. 1: (a) Diffusion coefficients determined from broadband dielectric spectra by employing the Einstein-Smoluchowski equation (using ω_c as the characteristic hopping rate) and independently measured by PFG NMR (open symbols). The lines denote fits by the Vogel-Fulcher-Tammann equation. Inset: One of the possible conformations of the [OMIM] cation. (b) The apparent activation energy, ΔG, of diffusivity in a series of bis(trifluoromethyl-sulfonyl)imide-based ionic liquids at different temperatures (determined from the VFT fits presented in Figure 2). ΔG increases with the mean ion jump lengths (indicated in brackets). Inset: The mean jump lengths (from a combination of broadband dielectric spectroscopy and PFG NMR measurements) as a function of the molecular volume (from quantum chemical calculations) of the ionic liquids investigated.

References:

[1] J. R. Sangoro *et al*., Diffusion in ionic liquids: the interplay between molecular structure and dynamics, Soft Matter (2011), in press. DOI:10.1039/ C0SM01404D

Collaborators: R. Buchner (University of Regensburg), V. Strehmel (Niederrhein University of University of Applied Sciences), J. Kärger (University of Leipzig), R. Valliulin (University of Leipzig)

Funding: DFG under the priority program SPP 1191 on “Ionic Liquids”

2.8 Charge transport and dipolar relaxations in metal-based ionic liquids

J. R. Sangoro, C. Iacob, W. K. Kipnusu, T. Schubert, and F. Kremer

Charge transport and dipolar relaxations in novel alkali metal-based carboxylate ionic liquids are investigated in a wide frequency and temperature range by means of Broadband Dielectric Spectroscopy (BDS) [1,2]. The dielectric spectra are described at lower temperatures in terms of dipolar relaxations whereas hopping conduction in a random spatially varying energy landscape is quantitatively shown to dominate the spectra at higher temperatures (see Fig. 1 (a)). Based on detailed analysis of the dielectric relaxation strength in its temperature dependence, the slower secondary relaxation process is attributed to molecular fluctuation of ion-pairs (sodium and carboxylate ions) while the localized motion of the carboxylate anion gives rise to the faster process observed (see Fig. 1 (b)). Experimental evidence for the existence of *long-lived ion pairs* in an ionic liquid is thus provided [2].

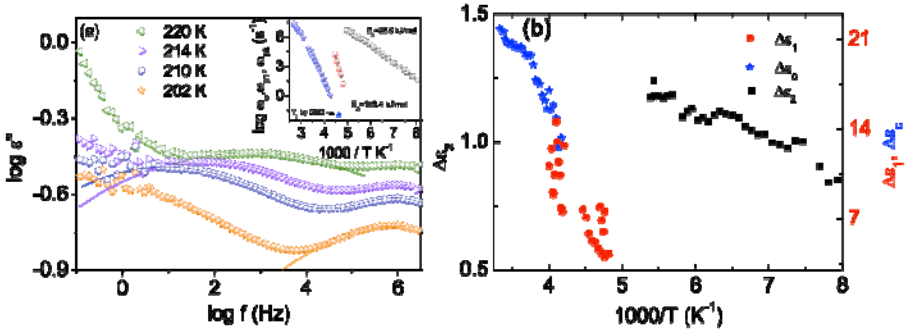

Fig. 1: (a) Imaginary part of the complex dielectric function *versus* frequency at different temperatures illustrating the secondary relaxation processes in the sodium 2,5,8,11-tetraoxatridecan-13-oate ([Na][TOTO]) ionic liquid. Inset: Arrhenius-type temperature dependence of the secondary relaxation rates ($1/\tau$) of [Na] [TOTO] at lower temperatures (114 K to 225 K). The activation energies are indicated. (b) The temperature dependence of the dielectric relaxation strength corresponding to charge transport $\Delta\varepsilon_c$ as well as the two secondary dipolar relaxations $\Delta\varepsilon_{\beta1}$ and $\Delta\varepsilon_{\beta2}$.

References:

[1] Zech, O. Hunger, J., Sangoro, J. R., Iacob, C., Kremer, F. Kunz, W., and Buchner, R. (2010). Correlation between polarity parameters and dielectric properties of [Na] [TOTO] – a sodium-based ionic liquid. *Phys. Chem. Chem. Phys.*, 12, 14341-14350.
[2] J. R. Sangoro *et al.*, Charge transport and dipolar relaxations in metal-based ionic liquids, Under preparation.

Collaborators: R. Buchner (University of Regensburg), P. Papadopolous (MPIP Mainz)

Funding: DFG under the priority program SPP 1191 on “Ionic Liquids”

2.13 Receptor/ligand-interaction as studied on a single molecule level

C. Wagner, D. Singer, R. Hoffmann and F. Kremer

Optical tweezers-assisted dynamic force spectroscopy is employed to investigate specific receptor/ligand-bonds on a single contact level. The specific binding of two monoclonal antibodies, HPT-110 and HPT-104, to synthetic tau-peptides with different phosphorylation pattern is analyzed. The specificity of HPT-110 to the tau-peptide containing a phosphorylation at Ser235 and of HPT-104 to the tau-peptide containing a phosphorylation at Thr231 is confirmed (Fig. 1 a). Additionally, our approach allows for a detailed characterization of the unspecific interactions that are observed between HPT-104 and the peptide phosphorylated only at Ser235 and between HPT-110 and the peptide phosphorylated only at Thr231. By analyzing the measured rupture-force distributions it is possible to separate unspecific from specific interactions. Thereby for the latter characteristic parameters like the lifetime of the bond without force τ_0, the characteristic length x_{ts} and the free energy of activation ΔG are determined (Fig. 1 b). The results are in accordance with conventional ELISA tests but offer a much more refined insight.

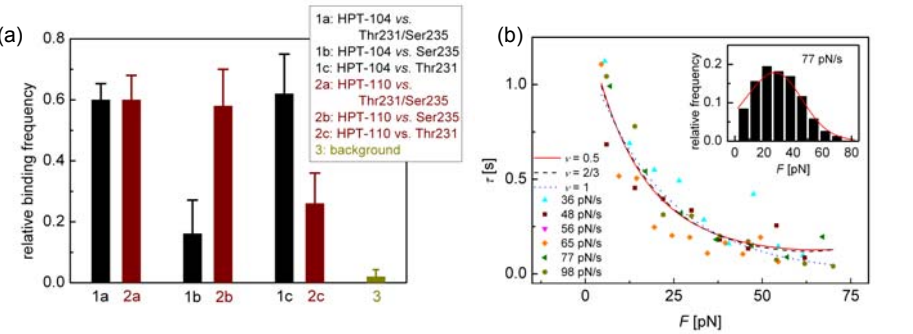

Fig. 1: a) The median relative binding frequency of each of the mAbs HPT-104 and HPT-110 to double-phosphorylated peptides and to peptides mono-phosphorylated at Thr231 and Ser235 is shown. The median frequency of both, HPT-104 and HPT-110 to the double-phosphorylated peptide is ~0.6. The binding frequency of HPT-104 to the peptide only phosphorylated at Thr231 is similar, whereas its binding frequency to the peptide phosphorylated at Ser235 is with ~0.25 significantly lower. For the mAb HPT-110 the result is vice versa: its binding frequency to the peptide mono-phosphorylated at Ser235 is significantly higher than to the peptide mono-phosphorylated at Thr231. The last column indicates the level of the “background”, which consists of interactions that are not caused by an interaction between receptor and ligand molecules. This “background” is with a binding frequency of <2% found to be negligible. b) The lifetime τ of the interaction between HPT-110 and the double-phosphorylated peptide is shown in dependence on the force for 6 different loading rates as indicated by the different symbols. The data is fitted globally to a well-known theoretical model. Inset: Histogram of the measured rupture forces at a loading rate of 77 pN. The red line indicates the theoretical distribution of rupture forces according to the theoretical model after inserting the parameters obtained by fitting $\tau(F)$.

References:

[1] M. Salomo et al., *Optical tweezers to study single protein A/immunoglobulin G interactions at varying conditions*, Eur Biophys J **37** (2008), 927-934
[2] C. Wagner et al., *The interaction of tau-peptides and monoclonal antibodies as studied by optical tweezers assisted dynamic force spectroscopy*, submitted to Soft Matter

Funding: Buildmona, Europäischer Sozialfonds (ESF)

2.12 Hierarchies in the structural organization of spider silk – A quantitative combined model

R. Ene, P. Papadopoulos, F. Kremer

Polarized IR-spectroscopic and mechanical measurements are combined to analyse the conformational changes in hydrogenated and partially deuterated major ampullate spider silk of Nephila edulis Fig.1a) [1]. Special attention is given to supercontraction and to the case where the latter is hindered by mechanical constraints. Crystal stress can be measured from the frequency shift of main-chain vibrations. The results show that in both states of silk a serial arrangement between the crystalline and amorphous phase dominates the nanostructure. The determination of the molecular order parameters of the different moieties proves that the amide hydrogen exchange is a selective process, taking place at the surface of β-sheet nanocrystals, implying that these regions are accessible by water [2]. The mechanical properties are changing dramatically when the fiber is wet ("supercontraction") due to the fact that the pre-stress of the chains interconnecting the nanocrystals is irreversibly released. In course of this a novel network of H-bonds is formed, a process which can be suppressed if supercontraction is hindered. A three-component combined model of crystals in serial arrangement with amorphous chains and a fraction of chains bypassing them can describe all states of spider silk, assuming hydrogen bonding of worm-like chains at low pre-strain Fig.1b) [3].

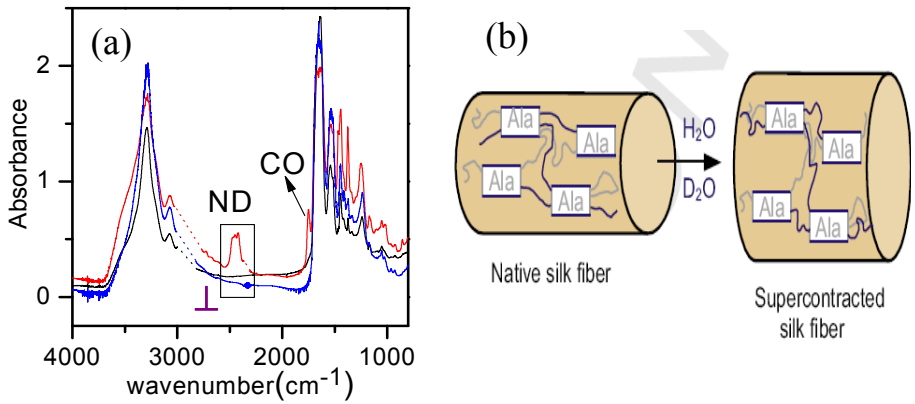

Fig.1 (a) IR absorption spectrum of major ampullate silk from *Nephila edulis* in native state (black curve) and supercontracted state (H_2O-blue curve and D_2O-red curve). The spectral region highlighted in the rectangle contains the ND bands resulted from the exchange of hydrogen with deuterium, (b) Accessibility of silk proteins to water. The exchange of amide hydrogens takes place primarily at highly ordered moieties, including amorphous chains with high pre-strain and possibly parts of the alanine nanocrystal surface (marked with blue).

References:

[1] P. Papadopoulos, R. Ene, I. Weidner, F. Kremer; Macromol. Rapid Commun 30, 851-857 (2009).
[2] R. Ene, P. Papadopoulos, F. Kremer; Polymer 51, 4784-4789 (2010)
[3] R. Ene, P. Papadopoulos, F. Kremer; Soft Matter 5, 4568-4574 (2009)

Funding: Graduate School BuildMoNa

2.9 Charge transport in confined ionic liquids

C. Iacob, J. R. Sangoro and F. Kremer,

Charge transport in tetrafluoroborate (BF_4) and bis[trifluoromethylsulfonyl]imide (NTf_2) based ionic liquids (ILs) in nanoporous silica membranes (average diameters: 7.5, 9.5 and 10.4 nm) – prepared by electrochemical etching of (100) p-type silicon - is investigated in a wide frequency and temperature range by a combination of Broadband Dielectric Spectroscopy (BDS) and Pulsed Field Gradient Nuclear Magnetic Resonance (PFG NMR) [1,2]. By applying the Einstein-Smoluchowski relation to the dielectric spectra, diffusion coefficient is obtained in quantitative agreement with independent PFG NMR measurements (Fig.1.A) (our PFG-NMR data are in agreement with the results reported by Bogno *et al.*). We experimentally show for the first time that the ionic mobility of the studied ILs at lower temperatures is enhanced by more than two decades under nanoconfinement geometry in comparison with the bulk value. The results are interpreted in terms of changes in the ion packing under condition of geometrical confinement.

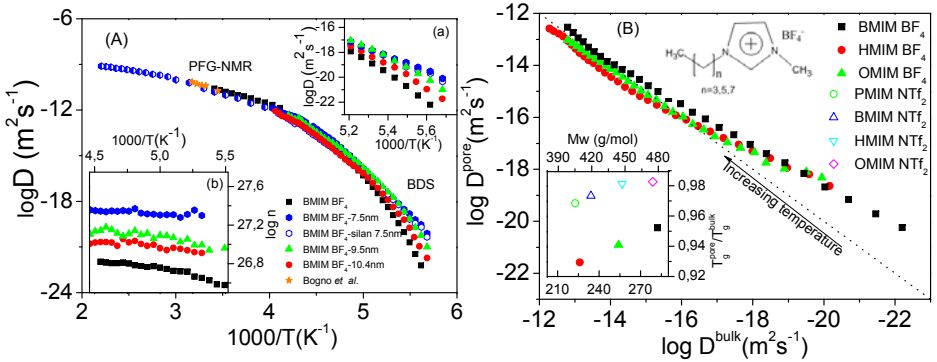

Fig.1: (A) Diffusion coefficients determined by applying the Einstein-Smoluchowski equation to the dielectric spectra of BMIM BF_4 (in bulk and nanopores denoted by filled symbols) and measured by PFG NMR (represented by half filled symbols).The star symbols represent the experimental diffusion coefficients using DOSY NMR from Bogno *et al.*, witch are in a good agreement with our PFG NMR and BDS measurements [3]. Inset: (a) enlargement of the spectra at lower temperatures and (b) effective number density of charge carriers of BMIM BF_4 in silica membranes with different pore sizes as a function of inverse temperature. (B) Diffusion coefficients of BF_4 – based ionic liquids in 7.5nm silica nanopores *versus* bulk diffusion coefficients. Arbitrary doted line represents 1:1 ratio between diffusion coefficients in pores and in bulk. Insets: Molecular weight for the BF_4 - and NTf_2 – based ionic liquids as a function of the ratio of the glass transition temperatures in pores, and bulk respectively. The structure of BF_4-based ionic liquids is indicated.

References:

[1] C.Iacob, J.R.Sangoro, P. Papadopoulos, T.Schubert, S. Naumov, R. Valluilin, J. Kärger, and F. Kremer, *Phys. Chem. Chem. Phys*., 12, (2010), 13798-13803.
[2] C. Iacob, J. R. Sangoro, J. Kärger and F. Kremer, *under preparation.*
[3] A. Bogno, F. D'Amico and G. Saielli, *J.Mol.Liq.*131-132 (2007), 17-23

Collaborators:

J. Kärger, R. Valiullin, S. Naumov (U Leipzig), M. Alexe (MPI, Halle), D.Hirsch (IOM, Leipzig)

Funding: Financial support from DFG (Germany) and NOW (The Netherlands) within IRTG "Diffusion in Porous Materials" and DFG Priority Program SPP1191 on Ionic Liquids is gratefully acknowledged.

2.10 Liquid crystals in confining geometry

M. Jasiurkowska, C. Iacob, P. Papadopoulos, F. Kremer, M. Massalska-Arodź

The molecular dynamics of 4-heptan-4'- isothiocyanatobiphenyl (abbreviated as 7BT) in confinement of cylindrical nanopores is studied by means of Broadband Dielectric Spectroscopy (BDS). In bulk, the investigated compound shows only one liquid crystalline phase [1,2], the highly ordered smectic E (SmE) phase, characterised by the orthorhombic arrangement of molecules within the layers. The confinement leads to modification of the dynamics of the molecular motion. The relaxation process around short axis (δ-relaxation) is faster in the pore than in the bulk and its temperature dependence is described by Arrhenious formula. The value of activation energy of the δ-relaxation is slightly higher for sample into pores then this obtained for a bulk of the SmE phase. The second process attributed to a librational motion of the molecules appears in the relaxation rates two decades faster then δ-relaxation. With decreasing temperature both processes merge and their sum follows the temperature curve of the II process. The crystallization temperature is significantly reduced in comparison to the value for bulk and it dependence on pores size.

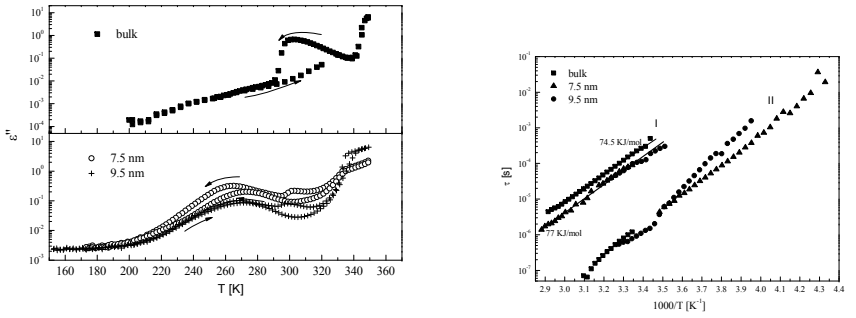

a) b)

Fig. 1: a) Dielectric loss ε'' for 7BT measured at 3.21 kHZ as a function of temperature on cooling and subsequent heating of the bulk sample and in pores of 7.5 nm and 9.5 nm. b) The activation pot, relaxation process I corresponds to δ-relaxation, process II is assigned to the librational motion of the molecules close to walls.

References

[1] M.Jasiurkowska, A. Budziak, J. Czub, M. Massalska-Arodź, S. Urban, Liq. Cryst. 2008, 35, 513
[2] M. Jasiurkowska, J. Ściesiński, M. Massalska-Arodź, J. Czub, R. Pełka, E Juszyńska, Y. Yamamura, K. Saito, J. Phys. Chem. B 2009, 113, 7435.

Collaborators:

Prof. Dr Maria Massalska Arodź (The Henryk Niewodniczanski Institute of Nuclear Physics Polish Academy of Sciences, Kraków)

Funding: Financial support by the Alexander von Humboldt Foundation is gratefully acknowledged.

2.11 Infrared transition moment orientational analysis (IR-TMOA)

W. Kossack, P. Papadopoulos, F. Kremer

A novel spectroscopic approach has been developed, that reveals a complete characterization of the quadratic averaged orientation of the different infrared transition dipole moments in any IR-translucent material. Using a rotary measurement setup, the electric field in the sample can be varied in all three dimensions (see inset). Since, the absorption coefficient is explicitly dependent on the relative orientation of the transition dipoles and the electric polarization (see Figure), one is enabled to quantify the fraction of ordered molecular moieties and their orientation [1]. Based on this technique thin, substrate supported, polymer films are studied in order to investigate their interaction with solid-state interfaces according to their specificity and range for different combinations of polymers and substrates, addressing the recent question of confinement and its extension.

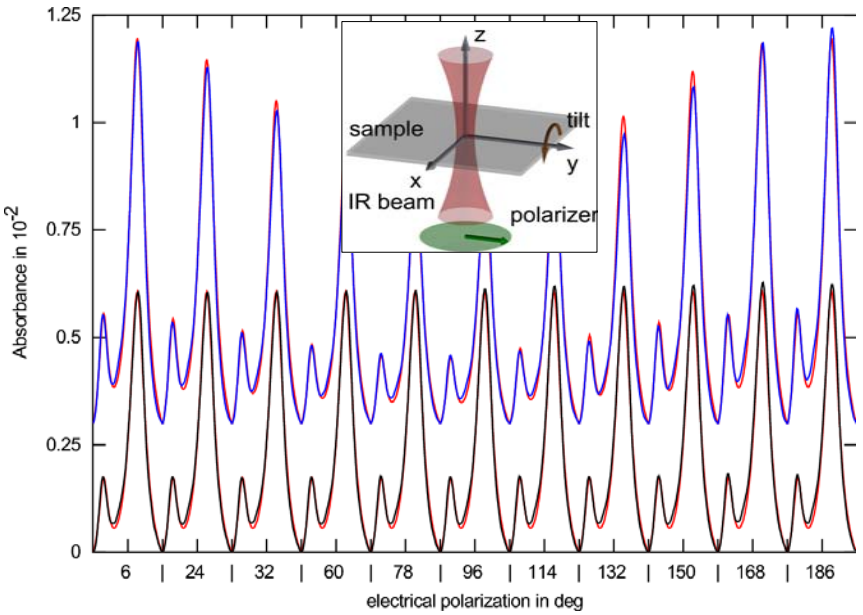

Fig. 1: Polarization (with respect to the *y* axis) and inclination (tilt) dependence of baseline corrected CH_2 stretching vibrations of polystyrene (~40 nm) on BaF_2. For comparison the bands for different electrical polarizations are put next to each other: The *x* axis shows wavenumbers from 2833 to 2981cm^{-1} for each polarization (between each two upright lines). The small peaks correspond to symm. CH_2 stretching (2850 cm^{-1}), the big peaks to asymm. CH_2 stretching (2920 cm^{-1}). The black and blue lines show the spectra for 0° and 60° inclination, where the latter is shifted by 0.3x10^{-2} units upwards. The red lines are the corresponding fits. As expected absorption shows no polarization dependence for normal incidence, where the 60° incidence spectra vary symmetrically around 90° polarization direction. The inset shows the measurement geometry.

References:

[1] Kossack, W., Papadopoulos, P., Heinze, P., Finkelmann, H., Kremer, F., Macromolecules 2010, 43, 7532–7539

Funding: Leipzig School of Natural Sciences, ''Building with Molecules and Nano-Objects'' (BuildMoNa)